

# CircMYH9 promotes the mRNA stability of SPAG6 by recruiting EIF4A3 to facilitate the progression of breast cancer

Shanji Fan<sup>a</sup>, Ying Cui<sup>b</sup>, Yingjie Liu<sup>a</sup>, Yuehua Li<sup>c</sup>, Hong Huang<sup>d,e</sup>, and Zecheng Hu<sup>a</sup>

<sup>a</sup>Department of Breast and Thyroid Surgery, The First Affiliated Hospital, Hengyang Medical School, University of South China, Hengyang, China; <sup>b</sup>College of Chemistry and Materials Science, Hengyang Normal University, Hengyang, Hunan, China; <sup>c</sup>Department of Medical Oncology, The First Affiliated Hospital, Hengyang Medical School, University of South China, Hengyang, China; <sup>d</sup>Institute of Cardiovascular Disease, The First Affiliated Hospital, Hengyang Medical School, University of South China, Hengyang, Hunan, China; <sup>e</sup>Hunan Provincial Key Laboratory of Multi-omics and Artificial Intelligence of Cardiovascular Diseases, University of South China, Hengyang, Hunan, China

## ABSTRACT

The incidence rate of breast cancer (BC) ranks first among female malignant tumors. Late-stage BC patients are at risk of death from distant metastasis. Circular RNAs (circRNAs) play an important function in cancer development. This study looked at the role of circMYH9 in BC. The nude mouse tumor-bearing experiment was used to verify the role of circMYH9 in regulating BC tumor growth in mice. Gene expression and protein amount were tested by qRT-PCR, western blot, and IHC. The pathological changes in tumor tissues were analyzed by HE staining. Cell viability, proliferation, migration, and invasion were assessed using CCK8, colony formation assay, wound healing assay, and Transwell assay, respectively. The interactions between circMYH9, SPAG6, and EIF4A3 were analyzed by RIP assay. CircMYH9 was significantly upregulated in BC, and its upregulated was related to poor prognosis. CircMYH9 silencing markedly impaired BC cell proliferation, migration, and invasion. Mechanistically, circMYH9 promoted the mRNA stability and expression of SPAG6 by recruiting EIF4A3. As expected, SPAG6 overexpression abrogated inhibition mediated by circMYH9 knockdown on BC cell malignant behaviors. In addition, circMYH9 knockdown inhibited PI3K/Akt signal pathway by increasing PTEN expression in BC cells, while was reversed by SPAG6 upregulation. PTEN inhibition abolished inhibition induced by circMYH9 downregulation on BC malignant progression. Moreover, circMYH9 silencing inhibited tumor growth in mice. CircMYH9 overexpression regulated the PTEN/PI3K/AKT pathway by increasing SPAG6 mRNA stability through recruiting EIF4A3, thereby promoting BC malignant progression.

## ARTICLE HISTORY

Received 10 July 2024  
Revised 12 March 2025  
Accepted 17 March 2025



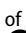


## KEYWORDS

Breast cancer; circMYH9; SPAG6; EIF4A3; the PTEN/PI3K/AKT pathway

## Introduction

Breast cancer (BC) is the most frequent cancer in women across the world [1]. As reported, about 2.26 million cases of BC were diagnosed globally in 2020, accounting for 24.5% of all female malignant tumor cases [2]. Although the prognosis of BC patients is good due to the latest advances in early diagnosis and effective treatment, recurrence or metastasis still poses a threat to survival [3]. As a result, novel diagnostic and treatment techniques are urgently needed to increase the efficiency of BC diagnosis and treatment, and exploring the molecular mechanism of BC and finding its prognostic markers and treatment targets is the key to achieving this goal.

Circular RNAs (circRNAs) are a new kind of RNA with a covalently closed loop structure [4]. CircRNAs are resistant to exonuclease because of their loop shape, making them significantly more durable than their mother linear RNAs and abundant in mammalian cells [5]. CircRNA dysregulation is a key risk factor promoting BC progression, as evidence, hsa\_circ\_001783 upregulation markedly promoted BC cell proliferation and invasion [6]. CircMYH9 (hsa\_circ\_0092283), as an intron-derived circRNA, originates from the MYH9 gene (22q12.3) and is located in chr22 (36681395--36681695). A previous study showed that circMYH9 upregulation was correlated with shorter overall survival of colorectal cancer

**CONTACT** Hong Huang  [trave1@126.com](mailto:trave1@126.com)  Institute of Cardiovascular Disease, The First Affiliated Hospital, Hengyang Medical School, University of South China, Hengyang 421000, Hunan, China; Zecheng Hu  [13875710120@163.com](mailto:13875710120@163.com)  Department of Breast and Thyroid Surgery, the First Affiliated Hospital, Hengyang Medical School, University of South China, No. 69 Chuanshan Road, Shigu District, Hengyang 421000, Hunan, China  
 Supplemental data for this article can be accessed online at <https://doi.org/10.1080/15592294.2025.2482382>

© 2025 The Author(s). Published by Informa UK Limited, trading as Taylor & Francis Group.

This is an Open Access article distributed under the terms of the Creative Commons Attribution-NonCommercial License (<http://creativecommons.org/licenses/by-nc/4.0/>), which permits unrestricted non-commercial use, distribution, and reproduction in any medium, provided the original work is properly cited. The terms on which this article has been published allow the posting of the Accepted Manuscript in a repository by the author(s) or with their consent.

patients [7]. Nonetheless, the role of circMYH9 in BC is not well understood and needs further research.

CircRNAs' underlying mechanics are complicated. CircRNAs control the expression of target genes by sponging numerous RNA-binding proteins (RBPs) [8]. Eukaryotic translation initiation factor4A3 (EIF4A3) is an RBP that is essential for RNA splicing, trafficking, translation, degradation, and positioning [9]. EIF4A3 is involved in the progression of multiple diseases, including cancers [10]. As proof, EIF4A3-induced circBRWD3 promoted BC tumorigenesis [11]. Notably, it was previously described that hsa\_circ\_0068631 facilitated BC development by binding to EIF4A3 [12]. Herein, bioinformatic prediction revealed that circMYH9 had possible binding sites for EIF4A3. Nevertheless, the interaction between circMYH9 and EIF4A3 in regulating BC development is still unknown.

Sperm-associated antigen 6 (SPAG6) was discovered in human testicular tissue for the first time, and functions in cooperating in germ cell development and preserving sperm viability and fertility [13]. SPAG6 dysregulation has a profound impact on multiple human malignant tumors [14,15]. A previous study identified SPAG6 as a novel biomarker for early BC detection [16]. In the present research, we predicted high confidence in the mRNA binding between EIF4A3 and SPAG6 through bioinformatics analysis. However, further research is needed to determine whether EIF4A3 can regulate the progression of BC by regulating the stability of SPAG6 mRNA. SPAG6 could promote Burkitt lymphoma cell proliferation and inhibit apoptosis by regulating the PTEN/PI3K/AKT pathway [17]. PTEN/PI3K/AKT is an essential signaling system that regulates apoptosis, cell proliferation, and cell growth [18]. The dysregulation of PTEN/PI3K/AKT signaling in tumors confers tumorigenic properties in several cellular systems [18]. In addition, the dysregulation of PTEN/PI3K/AKT signaling contributes to tumor cell metastasis and invasion [19]. Therefore, it is speculated that the SPAG6 upregulation promotes BC malignant progression by regulating the PTEN/PI3K/AKT pathway.

Collectively, it's speculated that circMYH9 upregulation regulated the PTEN/PI3K/AKT

pathway by increasing SPAG6 mRNA stability through recruiting EIF4A3, thus promoting BC cell proliferation and migration. As a result, circMYH9 May be a prognostic biomarker and might also serve as a potential therapeutic target for breast cancer patients. Our findings serve as a theoretical framework for the development of innovative BC treatment approaches.

## Materials and methods

### Clinical sample collection

According to the pathological stage, 50 BC tumor specimens and matched surrounding normal tissues were obtained from diagnosed BC patients post-operatively in the First Affiliated Hospital, Hengyang Medical School, University of South China. BC patients were not treated. Each participant completed a written informed consent form. The Ethics Committee of the First Affiliated Hospital, Hengyang Medical School, University of South China authorized the study. The detailed clinical and pathological information on the associated breast cancer patients were listed in Table S1.

### Cell culture and treatment

ATCC (VA, USA) provided the normal breast epithelial cells (MCF-10A cells) and human BC cell lines (T47D, BT474, MCF-7 and BT549 cells). All cells were grown in DMEM medium (Gibco, MD, USA) mixed with 10% FBS (Gibco) and 1% penicillin/streptomycin (Gibco) with 5% CO<sub>2</sub> at 37°C.

### Cell transfection

GenePharma (Shanghai, China) provide the short hairpin RNAs (sh-circMYH9 and sh-EIF4A3) and the overexpression plasmids (oe-circMYH9 and oe-SPAG6). The vectors were introduced into cells with Lipo3000 (Invitrogen, CA, USA).

### Immunohistochemistry (IHC)

After being deparaffinated and antigen retrieved (Dako, CA, USA), the tumor tissue slices (4 μm)

were blocked and treated overnight with antibodies against SPAG6 (Abcam, Cambridge, UK, 1:100, ab155653) and Ki67 (Abcam, 1:200, ab15580). The sections were then treated for 1 h with the secondary antibody (Abcam, 1:500, ab150077). The sections were reacted with DAB solution, stained with hematoxylin, dried, and sealed with neutral gum. The photos were captured in (Tokyo, Japan).

### **Cell counting kit-8 (CCK-8) assay**

Cells were cultured in 24-well plates ( $1 \times 10^4$  cells/well) for 24 h. Cells were then treated for 3 h with 10  $\mu$ L CCK8 solution (Sangon, Shanghai, China). The absorbance at 450 nm was measured.

### **Colony formation assay**

Cells were cultured in 6-well plates (1000 cells/well) for 7 d, fixed with methanol for 10 min, and stained with crystal violet (1%) for 5 min. The number of colonies was counted using an Olympus microscope.

### **Wound healing assay**

Cells were grown in 6-well plates ( $5 \times 10^5$  cells/well) for 12 h. Following removal of the media, a sterile pipette tip was used to construct an artificial wound. Cells were washed, cultured, and pictures were captured at 0 and 24 h.

### **Transwell invasion assay**

Cells ( $1 \times 10^4$ ) were added in serum-free medium and plated into the upper chamber which was precoated with Matrigel (BD, NJ, USA), and complete DMEM (1000  $\mu$ L) was added in the bottom chamber. Cells in the top chamber were removed after 12 h, while cells in the bottom chamber were fixed and stained with 0.5% crystal violet. An Olympus microscope was used to image cells.

### **RNA binding protein immunoprecipitation (RIP) assay**

The total mRNA was incubated with EIF4A3 antibody (Abcam, 1:30, ab180573) or IgG antibody

(Abcam, 1:100, ab109489) and incubated with protein A/G magnetic beads (Millipore, MA, USA) for 1 h. RNA was purified and analyzed by qRT-PCR.

### **mRNA stability assay**

Cells ( $8 \times 10^4$ ) were incubated with 5 mg/mL actinomycin D (Sigma-Aldrich) for 0 h, 1h, 2 h, and 4 h. Then RNA was analyzed by qRT-PCR.

### **Quantitative real-time polymerase chain reaction (qRT-PCR)**

Total RNA was extracted using TRIzol (Invitrogen). cDNA synthesis was carried out using a reverse transcription kit (ThermoFisher Scientific). ThermoFisher Scientific's SYBR was used for qRT-PCR. GAPDH was used as the reference gene. The data were analyzed using  $2^{-\Delta\Delta CT}$  method. The primers used in the study were listed as follows (5'-3'):

circMYH9 (F): CTCATGCCCTCCAGCCAG  
 circMYH9 (R): GGTCCAAGGCCAGCTCTG  
 SPAG4 (F): TCTCCAGTAGTCTCTGAGGAGC  
 SPAG4 (R): CGGATGGAACAGACCTCCC  
 SPAG5 (F): TTGAGGCCCGTTTAGATACCA  
 SPAG5 (R): GCTTTCCTTGGAGCAATGTAGTT  
 SPAG6 (F): GCTTTGAAAAGGATTGCTGCTT  
 SPAG6 (R): CCACTACTGTCTGTGCTAACTCT  
 SPAG9 (F): CAAGGCGGATCTAAAGCTACC  
 SPAG9 (R): TTGGCGCATCTGTAACTTCA  
 EIF4A3 (F): GGGGCATCTACGCTTACGG  
 EIF4A3 (R): GCGATGACATCTCTCCCTTGA  
 GAPDH(F): AGCCCAAGATGCCCTTCAGT  
 GAPDH(R): CCGTGTTCTACCCCAATG

### **Western blot**

A BCA kit (ThermoFisher Scientific) was used to measure the proteins after they had been separated using RIPA (Beyotime). The total protein was isolated by 10% SDS-PAGE and transferred to a Millipore PVDF membrane. The membranes were blocked and incubated with antibodies against EIF4A3 (ab180573), SPAG6 (ab155653), PTEN (ab267787), PI3K (ab191606), p-PI3K (ab182651), AKT (ab8805), p-AKT (ab38449) and  $\beta$ -actin (ab8226), overnight, then hybridized for 60 min with the secondary antibody (ab7090).

The protein bands were visualized by ECL and quantified by Image J. All antibodies were purchased from Abcam and diluted according to the instructions.

### Animal experiments

Eighteen female nude mice (5-week-old) were obtained from SJA LABORATORY (Hunan, China). After acclimation for 1 week, the mice were randomly classified into three groups: Control, LR, sh-NC, and sh-circMYH9 (with 6 mice in each group). The mice were subcutaneously implanted with an estradiol pellet (0.72 mg/60 d slow release; Innovative Research, CA, USA). The next day,

0.1 mL PBS containing  $1 \times 10^6$  MCF-7 cells which stable transfected with sh-NC or sh-circMYH9 were injected subcutaneously in the axilla of mice. The tumor volume was calculated using the following formula:  $V = lw^2/2$  (l: length, w: width). Tumor volume and body weight were measured every 5 d. The mice were then euthanized after 21 d, and the tumor tissues were collected.

### Hematoxylin-eosin (HE) staining

The tumor tissue block was fixed in 4% paraformaldehyde overnight. The fixed tissue block was embedded in paraffin and cut to a thickness of 5  $\mu$ m. The sections were dehydrated in different

alcohol concentrations and stained with HE (Sigma-Aldrich). The sections were observed and photographed under the Olympus microscope.

### Data analysis

Three separate trials were the source of all data. The statistical data indicated as Mean $\pm$ SD were analyzed using GraphPad Prism 7.0. Student's t-tests were used to examine the differences between the two groups, while one-way ANOVA was conducted to compare differences among groups. The *p* values less than 0.05 were regarded as significant.

### Results

#### *CircMYH9 was highly expressed in BC, and its high level was associated with poor prognosis*

It was first observed that circMYH9 expression was much greater in BC tissues than in adjacent normal tissues (Figure 1(a)). In addition, its upregulation was linked to poor prognosis (Figure 1(b)). Our results also demonstrated that circMYH9 was over-expressed in BC cells (T47D, BT474, MCF-7 and BT549 cells) compared with normal breast epithelial cells (MCF-10A cells) (Figure 1(c)). Considering that the expression of circMYH9 was higher in MCF-7 and BT549 cells among all BC cell lines (Figure 1(c)), therefore these two BC cell lines were chosen for further investigations. Collectively,

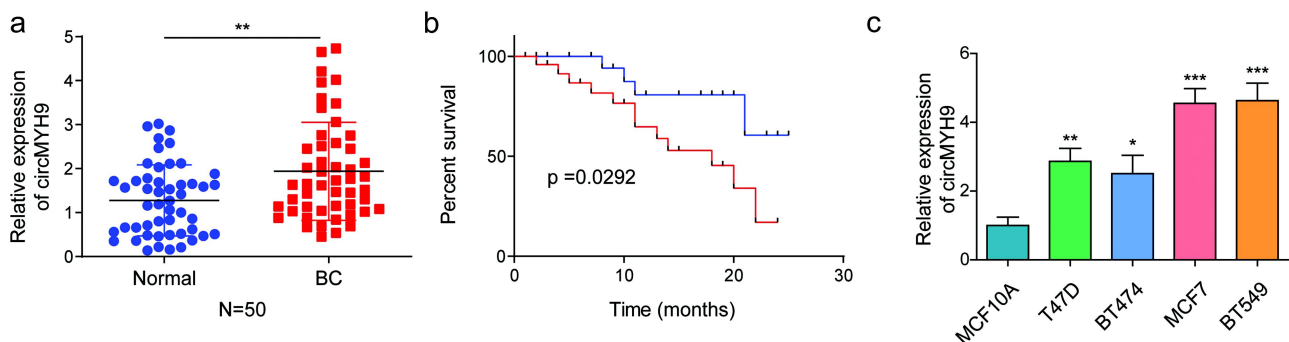


**Figure 1.** CircMYH9 was highly expressed in BC, and its high level was associated with poor prognosis of BC.

A total of 50 BC tumor tissues as well as paired adjacent normal tissues were collected post-operatively from BC patients. (a) CircMYH9 expression in tissues was detected by qRT-PCR. (b) Kaplan Meier survival analysis was used to analyze the relationship between circMYH9 expression and survival of BC patients. (c) qRT-PCR was employed to determine circMYH9 expression in BC cells (T47D, BT474, MCF-7 and BT549 cells) and normal breast epithelial cells (MCF-10A cells). The measurement data were presented as mean  $\pm$  SD. All data was obtained from at least three replicate experiments. \**p* < 0.05, \*\**p* < 0.01, \*\*\**p* < 0.001.



circMYH9 May play an important role in BC progression.

### ***CircMYH9 knockdown inhibited BC cell proliferation, invasion, and migration***

CircMYH9 knockdown was induced in MCF-7 and BT549 cells to study the role of circMYH9 in controlling BC development. It was firstly

observed that both sh-circMYH9-1 and sh-circMYH9-2 transfection significantly reduced circMYH9 expression level in MCF-7 and BT549 cells (Figure 2(a)). The knockdown efficiency of sh-circMYH9-1 was observed to be higher (Figure 2(a)), so sh-circMYH9-1 was selected for subsequent experiments. CCK8 assay subsequently showed that BC cell viability decreased with time after circMYH9 knockdown (Figure 2(b)). In

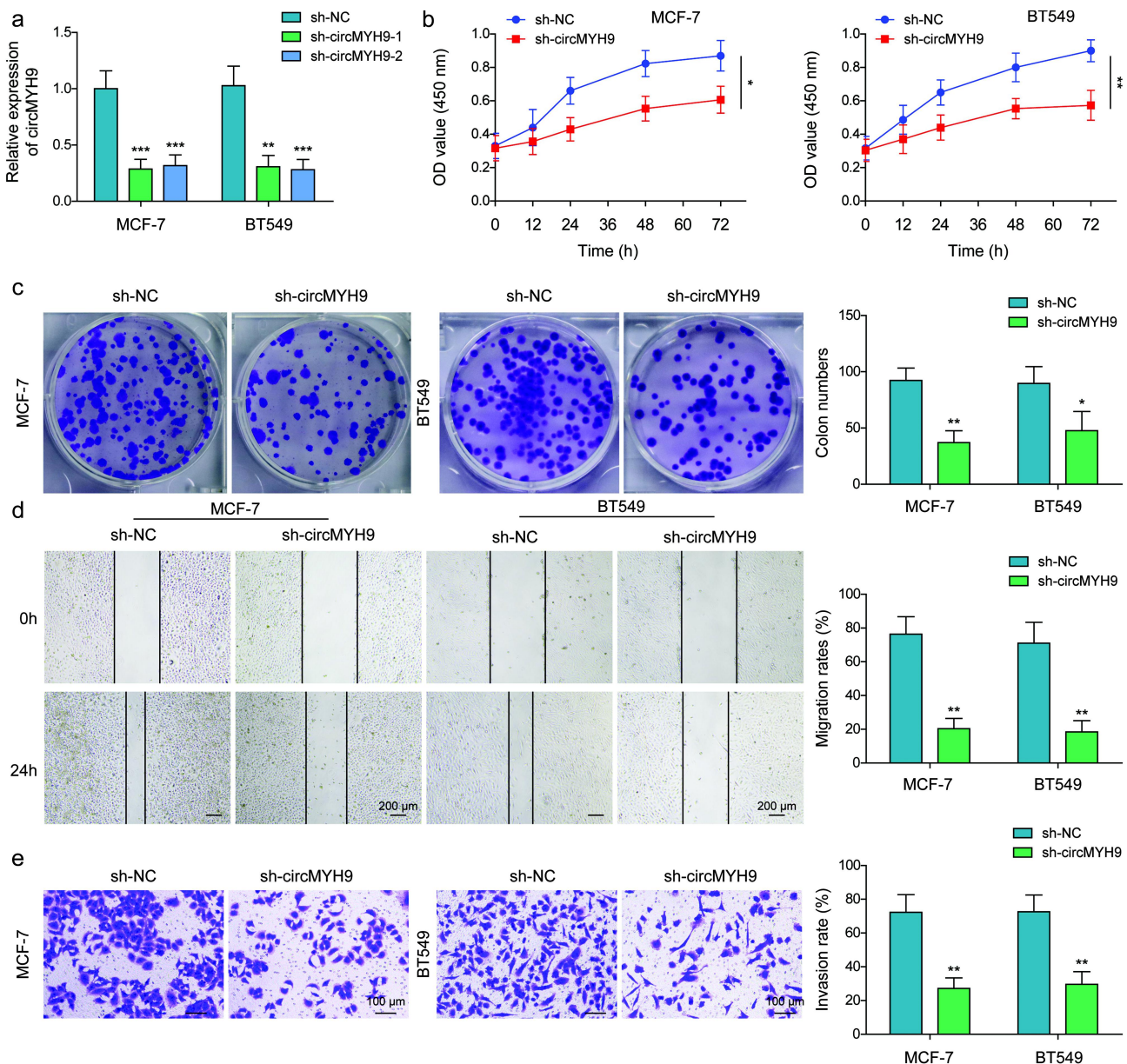


**Figure 2.** CircMYH9 knockdown inhibited BC cell proliferation, invasion, and migration.

(a) CircMYH9 expression in MCF-7 and BT549 cells after sh-NC, sh-circMYH9-1, or sh-circMYH9-2 transfection was examined by qRT-PCR. MCF-7 and BT549 cells were transfected with sh-NC or sh-circMYH9-1. (b) CCK8 assay was employed to determine cell viability. (c) Cell proliferation was detected by colony formation assay. (d) Cell migration was measured by wound healing assay (ruler 200  $\mu$ m). (e) Transwell assay was performed to examine cell invasion (ruler 100  $\mu$ m). The measurement data were presented as mean  $\pm$  SD. All data was obtained from at least three replicate experiments. \* $p$  < 0.05, \*\* $p$  < 0.01, \*\*\* $p$  < 0.001.

addition, circMYH9 silencing markedly inhibited BC cell proliferation (Figure 2(c)), invasion (Figure 2(d)) and migration (Figure 2(e)). Taken together, circMYH9 silencing suppressed BC cell malignant behaviors.

### **CircMYH9 expression was positively correlated with SPAG6 expression**

Before carrying out the research, we have detected the expressions of SPAG4, SPAG5, and SPAG9 in BC, and the correlation between the expression of these molecules and circMYH9 expression has also been analyzed. The results showed that both SPAG4, SPAG5, SPAG6, and SPAG9 were highly expressed in BC tissues than that in adjacent normal

tissues (Figure S1a). Among these SPAG proteins, the upregulation of SPAG6 was the most significant (Figure S1a). In addition, circMYH9 expression was positively correlated with the expression of SPAG4, SPAG5, SPAG6, and SPAG9 in clinical samples (Figure S1b). It was also observed that SPAG6 had the highest correlation with circMYH9 expression among these SPAG proteins (Figure S1b). SPAG6 is identified as a tumor marker [20]. As shown in Figure 3(a-b), SPAG6 expression was highly expressed in BC tissues. CircMYH9 expression was positively correlated with SPAG6 expression in clinical samples (Figure 3(c)). Meanwhile, SPAG6 expression was higher in BC cells compared with MCF-10A cells (Figure 3(d-e)). SPAG6 expression was higher in MCF-7 and BT549 cells among all BC

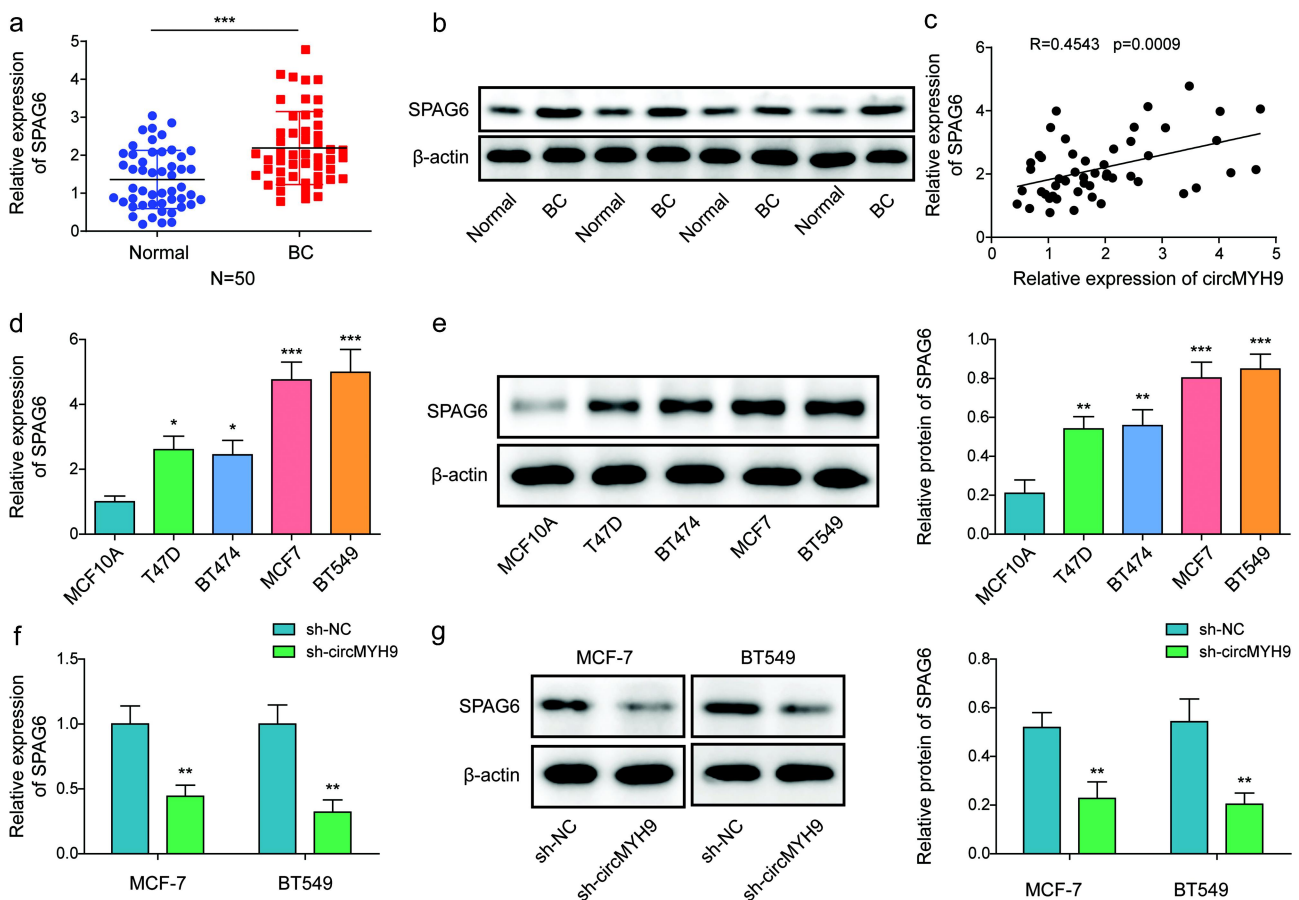


**Figure 3.** CircMYH9 expression was positively correlated with SPAG6 expression.

A total of 50 BC tumor tissues as well as paired adjacent normal tissues were collected post-operatively from BC patients. (a-b) The mRNA and protein levels of SPAG6 in tissues were examined by qRT-PCR and western blot. (c) Pearson correlation analysis was employed to analyze the correlation between circMYH9 and SPAG6. (d-e) The mRNA and protein levels of SPAG6 in BC cells (T47D, BT474, MCF-7, and BT549 cells) and normal breast epithelial cells (MCF-10A cells) were examined by qRT-PCR and western blot. (f-g) The mRNA and protein levels of SPAG6 in BC cells following sh-NC or sh-circMYH9 transfection were examined by qRT-PCR and western blot. The measurement data were presented as mean  $\pm$  SD. All data was obtained from at least three replicate experiments. \* $p < 0.05$ , \*\* $p < 0.01$ , \*\*\* $p < 0.001$ .

cell lines (Figure 3(d-e)). Moreover, it was observed that circMYH9 knockdown reduced SPAG6 expression levels in MCF-7 and BT549 cells (Figure 3(f-g)). In summary, circMYH9 positively regulated SPAG6 expression in BC cells.

### ***CircMYH9 increased SPAG6 mRNA stability by recruiting EIF4A3***

As widely described, circRNA regulates the mRNA stability of downstream targets by interacting with RBPs [21]. Herein, the CircInteractome database was utilized to predict the RBP interacting with circMYH9, and it was found that EIF4A3 was the most reliable RBP for interacting with circMYH9 (Figure 4(a)). As confirmed by RIP assay, circMYH9 directly interacted with EIF4A3 in BC cells (Figure 4(b)). In addition, SPAG6 directly interacted with EIF4A3, while this interaction was weakened by circMYH9 knockdown (Figure 4(c)). As shown in Figure 4(d), oe-circMYH9 transfection markedly elevated circMYH9 expression in BC cells. Meanwhile, both sh-EIF4A3-1, sh-EIF4A3-2, and sh-EIF4A3-3 transfection significantly reduced EIF4A3 expression level in MCF-7 and BT549 cells (Figure 4(e)). The knockdown efficiency of sh-EIF4A3-1 was observed to be higher (Figure 4(e)), so sh-EIF4A3-1 was selected for subsequent experiments. It was subsequently revealed that circMYH9 overexpression markedly elevated SPAG6 expression in BC cells, while these changes were eliminated by sh-EIF4A3 co-transfection (Figure 4(f-g)). Moreover, SPAG6 mRNA stability in BC cells was enhanced following circMYH9 upregulation, which was abolished after EIF4A3 downregulation (Figure 4(h)). In conclusion, circMYH9 increased SPAG6 mRNA stability and expression in BC cells by recruiting EIF4A3.

### ***CircMYH9 upregulation facilitated BC cell proliferation, invasion, and migration by upregulating SPAG6***

To explore the interaction between circMYH9 and SPAG6 in controlling BC development, both circMYH9 knockdown and SPAG6

overexpression were induced in MCF-7 and BT549 cells. It turned out that oe-SPAG6 transfection significantly increased SPAG6 mRNA level in BC cells (Figure 5(a)). Functional experiments subsequently showed that SPAG6 overexpression prevented sh-circMYH9-induced inhibition on BC cell viability (Figure 5(b)), proliferation (Figure 5(c)), invasion (Figure 5d) and migration (Figure 5(e)). In addition, circMYH9 silencing increased PTEN protein level but reducing p-PI3K and p-AKT levels in BC cells, while these protein expression changes were reversed by SPAG6 overexpression (Figure 5(f)). Collectively, circMYH9 upregulation promoted BC cell malignant behaviors by increasing SPAG6 expression.

### ***CircMYH9 facilitated BC cell malignant behaviors by regulating the PTEN/PI3K/AKT signaling pathway***

To investigate the interaction between circMYH9 and PTEN/PI3K/AKT signaling pathway in regulating BC development, circMYH9 knockdown was induced in MCF-7 and BT549 cells combined with SF1670 (PTEN inhibitor) treatment. As demonstrated in Figure 6(a), circMYH9 knockdown elevated PTEN protein levels but reduced p-PI3K and p-AKT levels in BC cells, whereas these changes were reversed by SF1670 treatment. It also turned out that sh-circMYH9-induced inhibition on BC cell viability (Figure 6(b)), proliferation (Figure 6(c)), invasion (Figure 6(d)), and migration (Figure 6(e)) were all abrogated by SF1670 treatment. All these results suggested that circMYH9 upregulation promoted BC cell malignant behaviors by regulating the PTEN/PI3K/AKT signaling pathway.

### ***CircMYH9 silencing inhibited tumor growth in mice***

The tumor implantations experiment was used to verify the effect of circMYH9 on BC malignant progression *in vivo*. As shown in Figure 7(a-c), circMYH9 knockdown markedly inhibited tumor growth in mice. In addition, circMYH9 knockdown significantly reduced circMYH9 expression in tumor tissues (Figure 7(d)). The results from



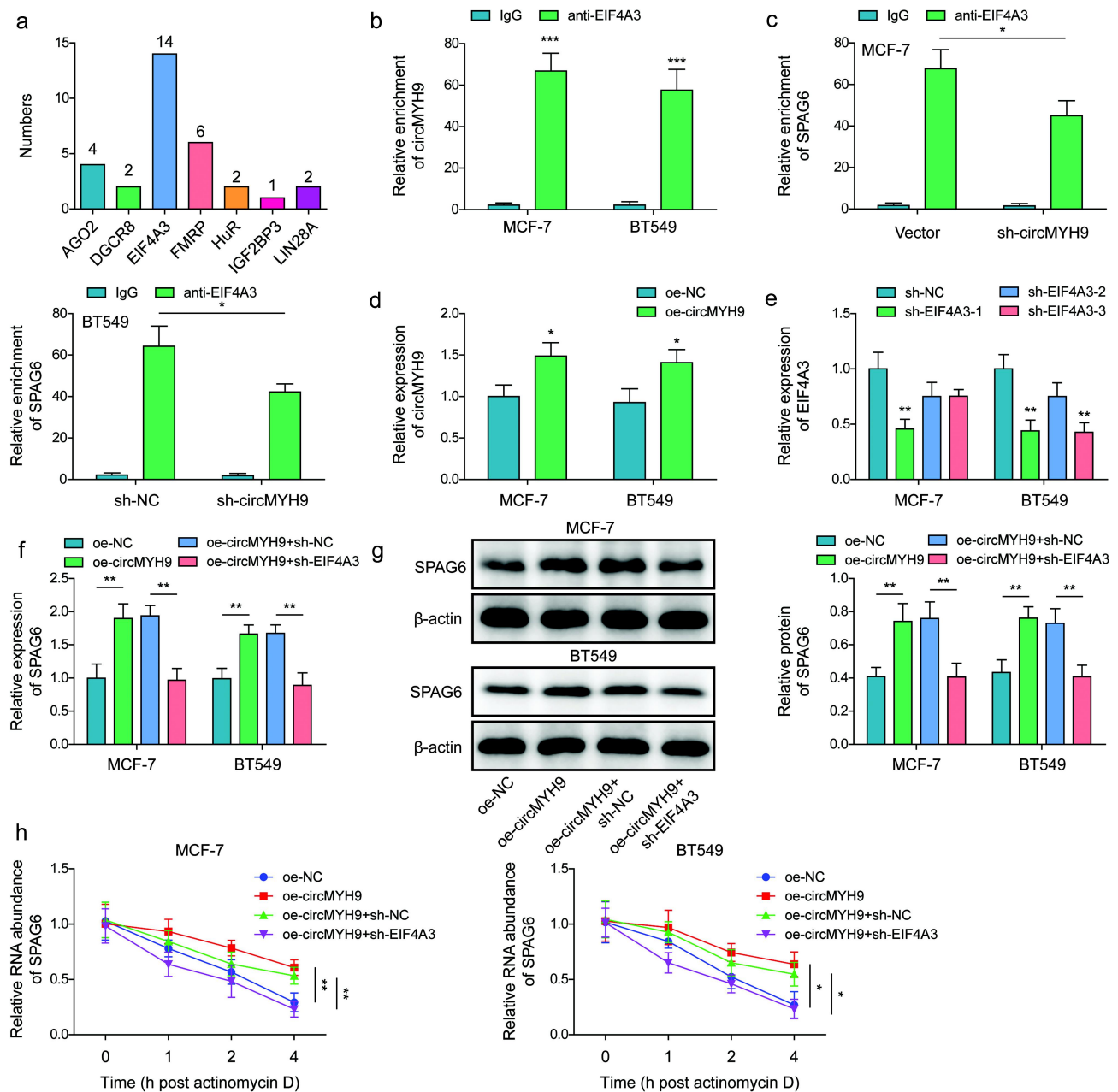


**Figure 4.** CircMYH9 increased SPAG6 mRNA stability by recruiting EIF4A3.

(a) The CircInteractome database was utilized to predict the RBP interacting with circMYH9. (b) The interaction between circMYH9 and EIF4A3 was analyzed by RIP assay. (c) The interaction between SPAG6 and EIF4A3 was analyzed by RIP assay. (d) CircMYH9 expression in BC cells after oe-NC or oe-circMYH9 transfection was detected by qRT-PCR. (e) EIF4A3 expression in BC cells after sh-NC, sh-EIF4A3-1, sh-EIF4A3-2, or sh-EIF4A3-3 transfection was determined by qRT-PCR. MCF-7 and BT549 cells were co-transfected with oe-circMYH9 and sh-EIF4A3. (f-g) The mRNA and protein levels of SPAG6 in cells were examined by qRT-PCR and Western blot. (h) SPAG6 mRNA stability was tested by mRNA stability assay. The measurement data were presented as mean  $\pm$  SD. All data was obtained from at least three replicate experiments. \* $p$  < 0.05, \*\* $p$  < 0.01, \*\*\* $p$  < 0.001.

HE staining and IHC subsequently showed that circMYH9 silencing markedly reduced tumor cell proliferation and the levels of KI67 and SPAG6 (Figure 7(e-f)). Moreover, circMYH9 knockdown significantly increased PTEN protein levels while

reducing p-PI3K and p-AKT levels in tumor tissues (Figure 7(g)). Taken together, circMYH9 knockdown inhibited BC tumor growth in mice by regulating the PTEN/PI3K/AKT pathway through increasing SPAG6 expression.



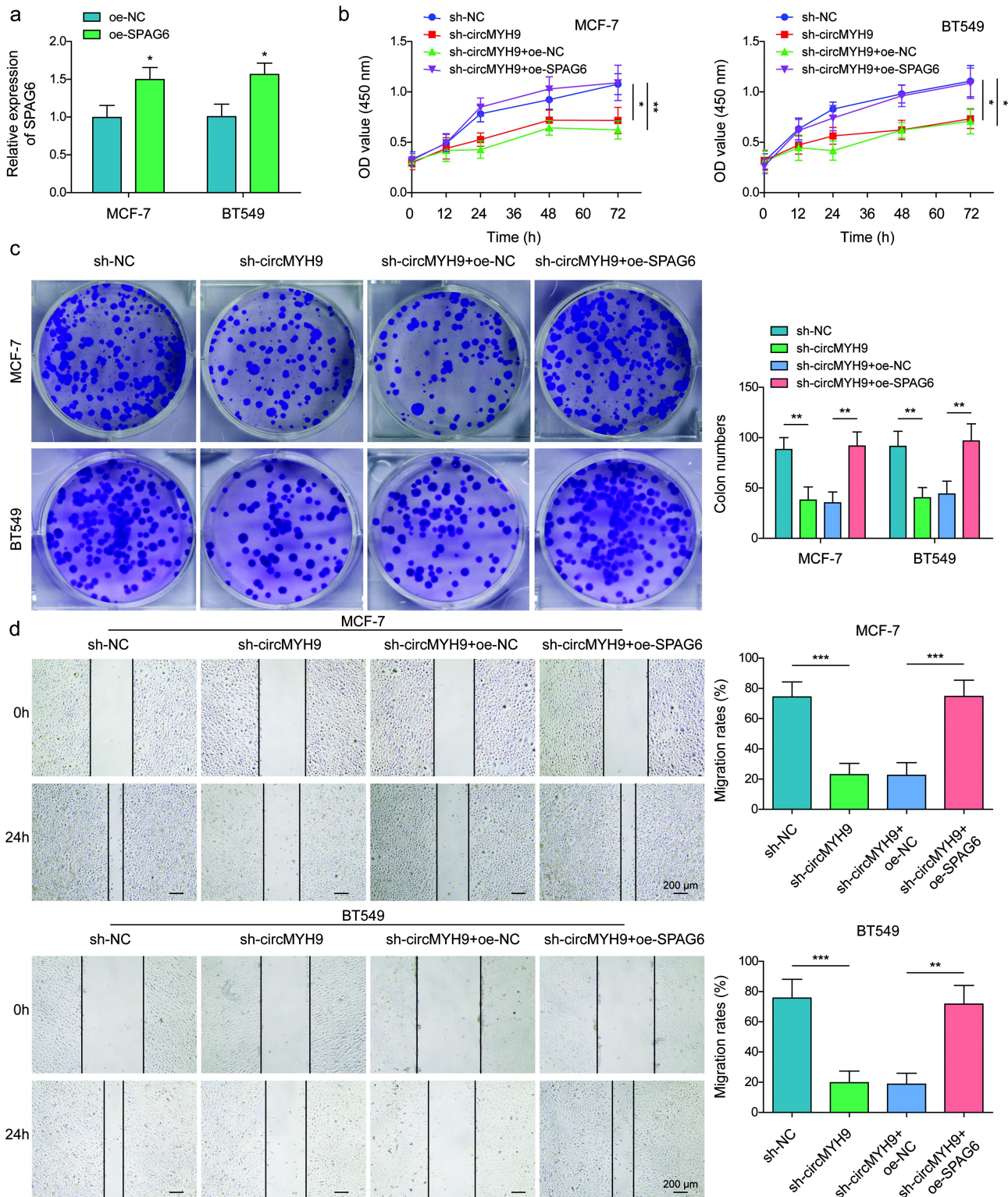


**Figure 5.** CircMYH9 upregulation facilitated BC cell proliferation, invasion, and migration by upregulating SPAG6.

(a) SPAG6 expression in BC cells after oe-NC or oe-SPAG6 transfection was detected by qRT-PCR. Both circMYH9 knockdown and SPAG6 overexpression were induced in MCF-7 and BT549 cells. (b) CCK8 assay was employed to determine cell viability. (c) Cell proliferation was detected by colony formation assay. (d) Cell migration was measured by wound healing assay (ruler 200  $\mu$ m). (e) Transwell assay was performed to examine cell invasion (ruler 100  $\mu$ m). (f) PTEN, PI3K, p-PI3K, AKT, and p-AKT protein levels in BC cells were measured by western blot. The measurement data were presented as mean  $\pm$  SD. All data was obtained from at least three replicate experiments. \* $p$  < 0.05, \*\* $p$  < 0.01, \*\*\* $p$  < 0.001.

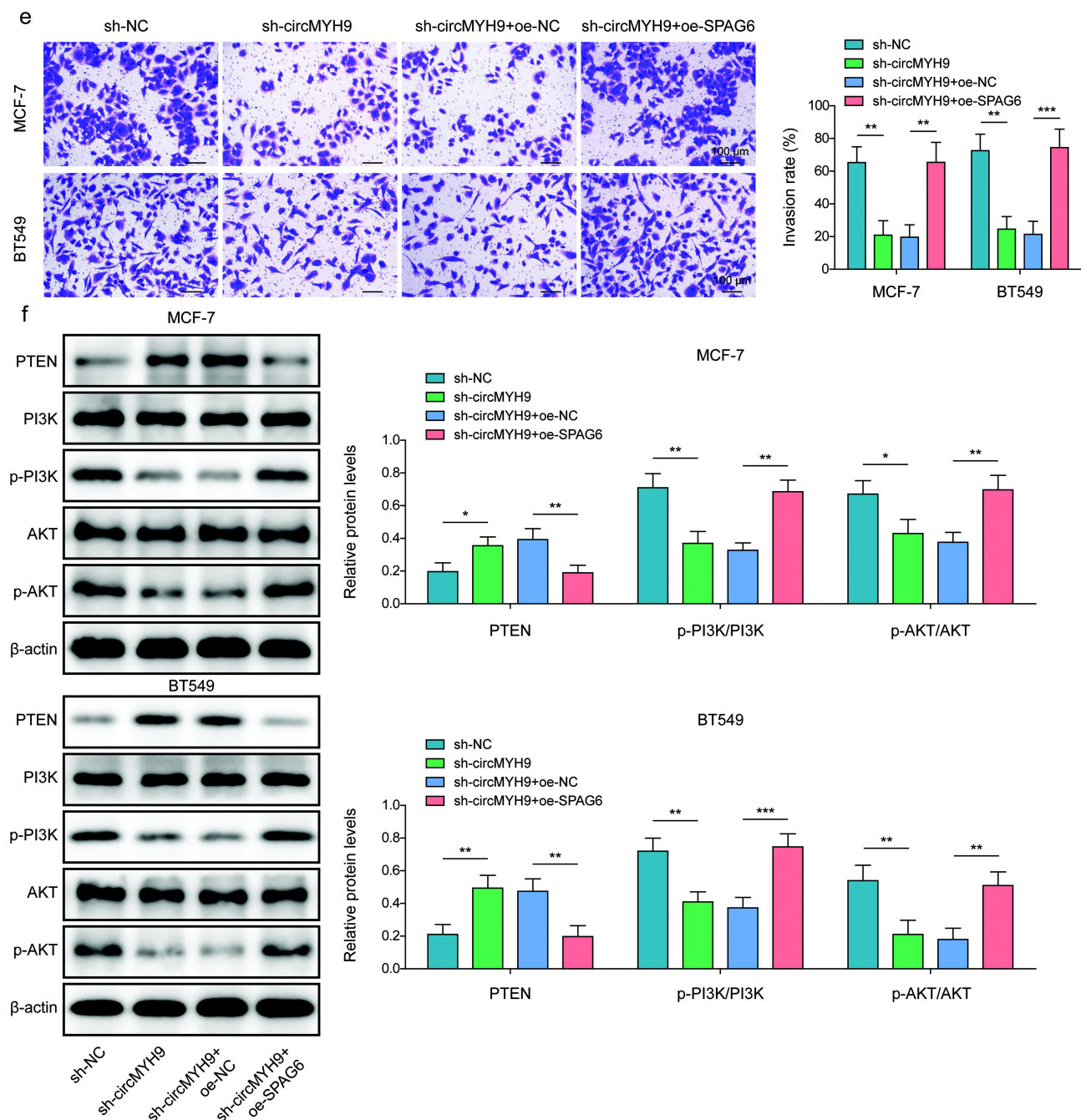


Figure 5. (Continued).

## Discussion

Breast cancer is the most often diagnosed cancer in women globally, as well as the leading cause of death [22]. Despite improvements in overall survival and prognosis for BC patients in recent years, metastasis remains the major cause of death in BC patients [23]. The 5-year survival rate for patients with metastases is just 26%, compared to 90% for all BC patients [24]. The underlying molecular pathways that

regulate BC metastasis and identify new treatment targets were studied in this study. The current study's key unique results are that circMYH9 upregulation regulated the PTEN/PI3K/AKT pathway by enhancing SPAG6 mRNA stability through interacting with EIF4A3, thereby facilitating BC cell proliferation, migration, and invasion.

Accumulating evidence has demonstrated that circRNAs play key roles in tumorigenesis.



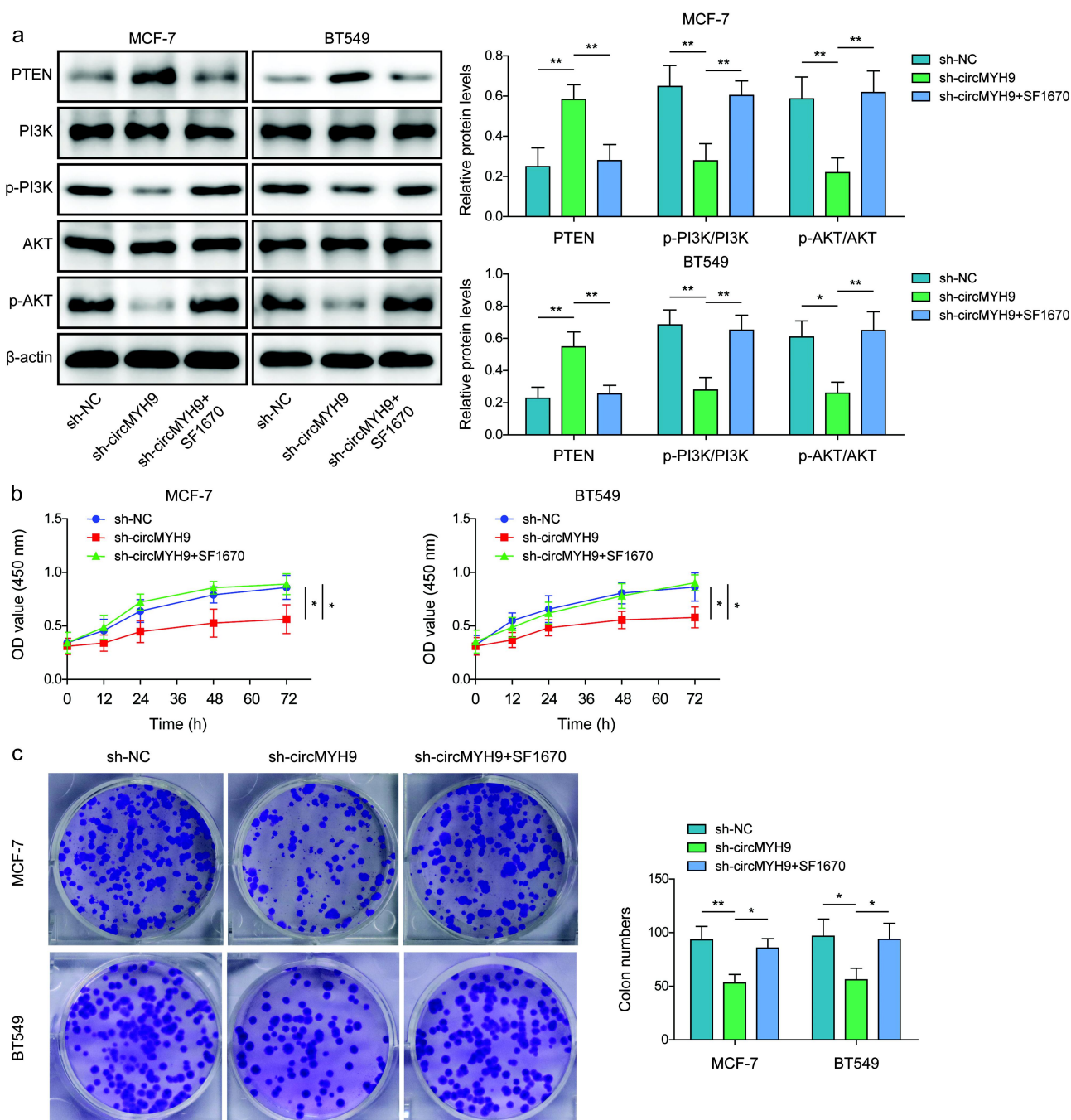


**Figure 6.** CircMYH9 facilitated BC cell malignant behaviors by regulating the PTEN/PI3K/AKT signaling pathway.

CircMYH9 knockdown was induced in MCF-7 and BT549 cells combined with SF1670 (PTEN inhibitor) treatment. (a) Western blot was adopted to detect PTEN, PI3K, p-PI3K, AKT, and p-AKT protein levels in BC cells. (b) CCK8 assay was performed to determine cell viability. (c) Cell proliferation was measured by colony formation assay. (d) Cell migration was measured by wound healing assay (ruler 200  $\mu$ m). (e) Transwell assay was performed to examine cell invasion (ruler 100  $\mu$ m). The measurement data were presented as mean  $\pm$  SD. All data was obtained from at least three replicate experiments. \* $p$  < 0.05, \*\* $p$  < 0.01, \*\*\* $p$  < 0.001.

CircRNAs are particularly essential due to their stable structure, which distinguishes them from other non-coding RNAs [25]. CircMYH9 was identified as a novel circRNA, which was over-expressed in multiple human malignant tumors,

such as colon cancer [7] and hepatocellular carcinoma [26]. The function of circMYH9 in BC hasn't been reported before. Herein, circMYH9 was overexpressed in BC tissues and cells, and its upregulation was related to BC patient poor

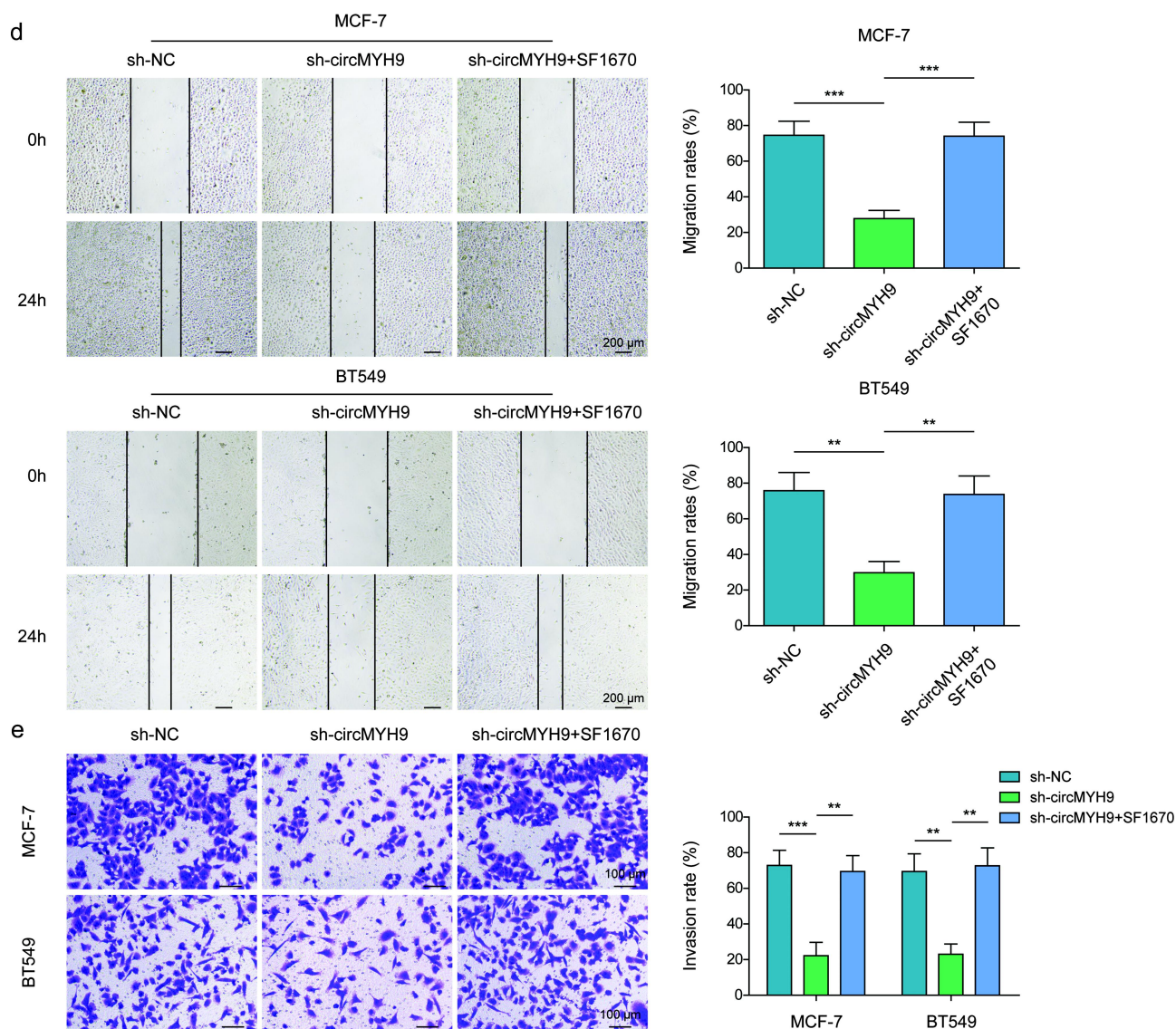


**Figure 6.** (Continued).

prognosis. In addition, circMYH9 silencing markedly inhibited BC cell proliferation, migration, and invasion. Moreover, circMYH9 knock-down inhibited tumor growth in mice. The mechanism by which circMYH9 regulated BC metastasis was subsequently studied. As widely reported, circRNAs may control the mRNA stability and expression downstream through binding to RBPs [27]. As proof, Xia et al. revealed that circMYH9 enhanced KPNA2 mRNA stability to accelerate hepatocellular carcinoma development by interacting with RBP EIF4A3 [26]. EIF4A3 is a vital modulator of RNA splicing [28]. Notably, it has been widely described that

EIF4A3 was highly expressed in BC [12,27]. CircMYH9 was observed to interact with EIF4A3 in this study. Therefore, all these results suggested that circMYH9 upregulation promoted BC cell malignant behaviors by recruiting EIF4A3.

SPAG6 is involved in germ cell maturation and flagella movement [29]. The quantity of research concentrating on the relationship between SPAG6 and cancer has significantly expanded during the last decade. As revealed by Zhang et al., SPAG6 upregulation facilitated Burkitt lymphoma cell proliferation [17]. In addition, SPAG6 overexpression is linked to the



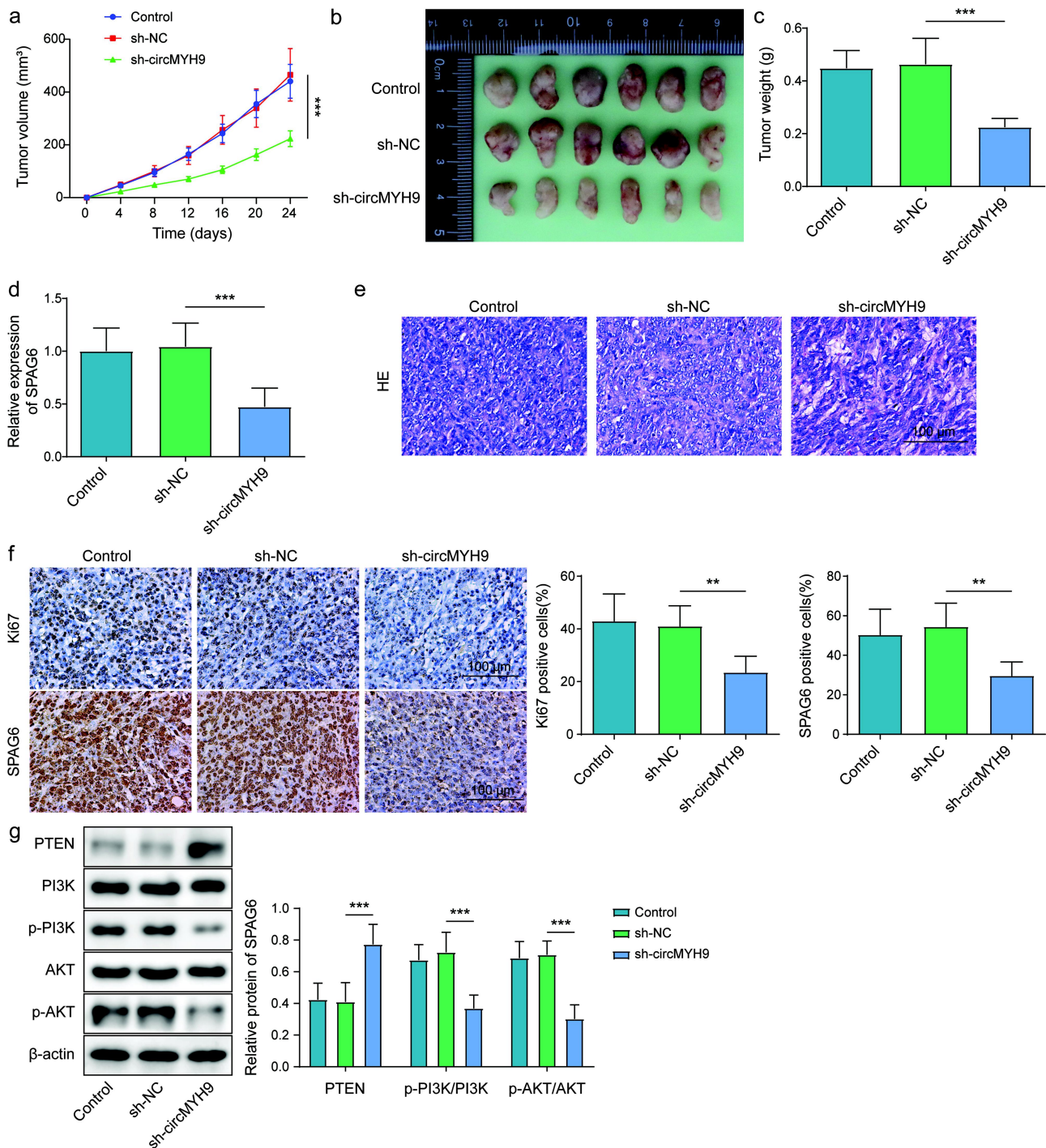


**Figure 7.** CircMYH9 silencing inhibited tumor growth in mice.

The tumor implantation experiment was performed. (a-b) The size, volume, and weight of tumors were measured. (c) CircMYH9 expression in tumor tissues was determined by qRT-PCR. (e) The pathological changes in tumor tissues were analyzed by HE staining (ruler 100 μm). (f) IHC was employed to detect Ki67 and SPAG6 protein levels in tumor tissues (ruler 100 μm). (g) PTEN, PI3K, p-PI3K, AKT, and p-AKT protein levels in tumor tissues were measured by western blot. The measurement data were presented as mean ± SD.  $n = 6$ . \* $p < 0.05$ , \*\* $p < 0.01$ , \*\*\* $p < 0.001$ .

clinical outcome of BC and lung cancer [20,30]. Our results showed that SPAG6 was overexpressed in BC. Before carrying out the research, we expressed a strong interest in the SPAG

proteins. The research found that the SPAG proteins have potential roles in cancer, but there are relatively few reports on their roles in BC. Therefore, we further screened the

SPAG proteins with potential carcinogenicity in BC. SPAG4 has recently been discovered as a novel cancer biomarker that has been shown to promote lung cancer cell migration [31]. SPAG5 has been proven to have carcinogenic effects in solid tumors, overexpressed in various cancers, and significantly associated with poor patient prognosis. It can be used as a diagnostic, prognostic survival marker, and immunotherapy target for multiple tumors [32–34]. Notably, a previous study showed that SPAG5 could be used as an independent prognostic and predictive biomarker that might have clinical utility in BC [35]. SPAG9 is overexpressed in multiple human malignant tumors, such as prostate cancer and liver cancer, and promotes tumor proliferation, invasion, and metastasis [36,37]. Our study found that SPAG6 had the highest correlation with circMYH9 expression among these SPAG proteins. Considering that SPAG6 has carcinogenicity in other cancers, its research in breast cancer is very limited. In addition, it was also observed that circMYH9 knockdown significantly reduced SPAG6 expression in BC cells, suggesting that circMYH9 may potentially regulate the expression of SPAG6 in BC cells. It also turned out that circMYH9 increased SPAG6 mRNA stability by recruiting EIF4A3. As expected, SPAG6 upregulation abolished inhibition mediated by circMYH9 knockdown on BC cell malignant behaviors. Taken together, circMYH9 upregulation promoted BC cell malignant behaviors by enhancing SPAG6 mRNA stability through recruiting EIF4A3.

PTEN and the associated PI3K/AKT pathway are critical in several activities, including stem cell differentiation and renewal, as well as oncogenesis [18]. Aberrant signaling of PTEN/PI3K/AKT has been revealed to be present in the majority of BC tumors, with multiple findings implicating this pathway in the start and progression of this cancer type [38,39]. Herein, the PTEN/PI3K/AKT pathway acted as the downstream pathway of circMYH9/SPAG6 axis in regulating BC progression. As expected, PTEN inhibition abrogated inhibition induced by circMYH9 knockdown on BC cell malignant behaviors. Collectively, circMYH9 overexpression facilitated BC cell

malignant behaviors by controlling the PTEN/PI3K/AKT pathway. In addition to the direct regulation of SPAG6 on the PTEN/PI3K/AKT pathway, it was important to consider other potential mechanisms through which SPAG6 could influence PTEN expression. According to a study by Yin et al. [40], SPAG6 regulated PTEN expression indirectly via DNA methylation. The authors suggested that SPAG6 upregulated DNA methyltransferase 1 (DNMT1) expression to enhance the methylation status of PTEN promoter region. This methylation process could lead to the silencing of PTEN expression, thereby contributing to the activation of the PI3K/AKT pathway and promoting tumor progression. This potential epigenetic regulation by SPAG6 provides further insight into the complex mechanisms underlying the modulation of PTEN expression in cancer cells, particularly in the context of breast cancer.

Our research proved that circMYH9 controlled the PTEN/PI3K/AKT pathway by boosting SPAG6 mRNA stability through recruiting EIF4A3, thereby promoting BC malignant development. These findings provide new targets for the diagnosis and treatment of BC. The results demonstrate that circMYH9 is an oncogene in BC, which may serve as a crucial marker of BC prognosis and may be a promising therapeutic target.

## Disclosure statement

No potential conflict of interest was reported by the author(s).

## Funding

This work was supported by grants from the Natural Science Foundation of Hunan Province [No. 2022JJ40393; 2023JJ60051], Project of Hunan Provincial Health Commission [No. 202204014247; W20243224].

## Authors' contributions

Shanji Fan: Conceptualization; Methodology; Writing – Original Draft;  
Ying Cui: Formal analysis; Investigation;  
Yingjie Liu: Data Curation; Resources;  
Yuehua Li: Validation; Project administration;  
Hong Huang: Visualization; Supervision;  
Zecheng Hu: Writing – Review & Editing; Funding acquisition

## Availability of data and materials

The datasets generated during and/or analyzed during the current study are available from the corresponding author upon reasonable request.

## Consent for publication

Each participant completed a written informed consent form.

## Ethics approval and consent to participate

The Ethics Committee of the the First Affiliated Hospital, Hengyang Medical School, University of South China authorized the study.

## Abbreviations

BC	Breast cancer
circRNAs	Circular RNAs
RBP	RNA-binding proteins
EIF4A3	Eukaryotic translation initiation factor4A3
SPAG6	Sperm-associated antigen 6
IHC	Immunohistochemistry
RIP	RNA binding protein immunoprecipitation
qRT-PCR	Quantitative real-time polymerase chain reaction

## References

- [1] Kalimutho M, Nones K, Srihari S, et al. Patterns of genomic instability in breast cancer. *Trends Pharmacol Sci.* 2019;40(3):198–211. doi: [10.1016/j.tips.2019.01.005](https://doi.org/10.1016/j.tips.2019.01.005)
- [2] Sung H, Ferlay J, Siegel RL, et al. Global cancer statistics 2020: GLOBOCAN estimates of incidence and mortality worldwide for 36 cancers in 185 countries. *CA Cancer J Clin.* 2021;71(3):209–249. doi: [10.3322/caac.21660](https://doi.org/10.3322/caac.21660)
- [3] Liang G, Ling Y, Mehrpour M, et al. Autophagy-associated circRNA circCDYL augments autophagy and promotes breast cancer progression. *Mol Cancer.* 2020;19(1):65. doi: [10.1186/s12943-020-01152-2](https://doi.org/10.1186/s12943-020-01152-2)
- [4] Chen L, Wang C, Sun H, et al. The bioinformatics toolbox for circRNA discovery and analysis. *Brief Bioinform.* 2021;22(2):1706–1728. doi: [10.1093/bib/bbaa001](https://doi.org/10.1093/bib/bbaa001)
- [5] Jeck WR, Sorrentino JA, Wang K, et al. Circular RNAs are abundant, conserved, and associated with ALU repeats. *RNA (New York, NY).* 2013;19(2):141–157. doi: [10.1261/rna.035667.112](https://doi.org/10.1261/rna.035667.112)
- [6] Liu Z, Zhou Y, Liang G, et al. Circular RNA hsa\_circ\_001783 regulates breast cancer progression via sponging miR-200c-3p. *Cell Death Dis.* 2019;10(2):55. doi: [10.1038/s41419-018-1287-1](https://doi.org/10.1038/s41419-018-1287-1)
- [7] Liu X, Liu Y, Liu Z, et al. CircMYH9 drives colorectal cancer growth by regulating serine metabolism and redox homeostasis in a p53-dependent manner. *Mol Cancer.* 2021;20(1):114. doi: [10.1186/s12943-021-01412-9](https://doi.org/10.1186/s12943-021-01412-9)
- [8] Xu S, Ge Y, Wang X, et al. Circ-USP9X interacts with EIF4A3 to promote endothelial cell pyroptosis by regulating GSDMD stability in atherosclerosis. *Clin Exp Hypertens (New York, NY: 1993).* 2023;45(1):2186319. doi: [10.1080/10641963.2023.2186319](https://doi.org/10.1080/10641963.2023.2186319)
- [9] Sakellariou D, Frankel LB. EIF4A3: a gatekeeper of autophagy. *Autophagy.* 2021;17(12):4504–4505. doi: [10.1080/15548627.2021.1985881](https://doi.org/10.1080/15548627.2021.1985881)
- [10] Jiang X, Guo S, Wang S, et al. EIF4A3-induced circARHGAP29 promotes aerobic glycolysis in docetaxel-resistant prostate cancer through IGF2BP2/c-Myc/LDHA signaling. *Cancer Res.* 2022;82(5):831–845. doi: [10.1158/0008-5472.CAN-21-2988](https://doi.org/10.1158/0008-5472.CAN-21-2988)
- [11] Meng X, Li W, Meng Z, et al. EIF4A3-induced circBRWD3 promotes tumorigenesis of breast cancer through miR-142-3p\_miR-142-5p/RAC1/PAK1 signaling. *BMC Cancer.* 2022;22(1):1225. doi: [10.1186/s12885-022-10200-7](https://doi.org/10.1186/s12885-022-10200-7)
- [12] Wang X, Chen M, Fang L. hsa\_circ\_0068631 promotes breast cancer progression through c-Myc by binding to EIF4A3. *Mol Ther - Nucleic Acids.* 2021;26:122–134. doi: [10.1016/j.omtn.2021.07.003](https://doi.org/10.1016/j.omtn.2021.07.003)
- [13] Sapiro R, Kostetskii I, Olds-Clarke P, et al. Male infertility, impaired sperm motility, and hydrocephalus in mice deficient in sperm-associated antigen 6. *Mol Cell Biol.* 2002;22(17):6298–6305. doi: [10.1128/MCB.22.17.6298-6305.2002](https://doi.org/10.1128/MCB.22.17.6298-6305.2002)
- [14] Mu J, Yuan P, Luo J, et al. Upregulated SPAG6 promotes acute myeloid leukemia progression through MYO1D that regulates the EGFR family expression. *Blood Adv.* 2022;6(18):5379–5394. doi: [10.1182/bloodadvances.2021006920](https://doi.org/10.1182/bloodadvances.2021006920)
- [15] Wu Q, Yan Y, Shi S, et al. DNMT3b-mediated SPAG6 promoter hypermethylation affects lung squamous cell carcinoma development through the JAK/STAT pathway. *Am J Transl Res.* 2022;14(10):6964–6977.
- [16] Mijnes J, Tiedemann J, Eschenbruch J, et al. SNiPER: a novel hypermethylation biomarker panel for liquid biopsy based early breast cancer detection. *Oncotarget.* 2019;10(60):6494–6508. doi: [10.18632/oncotarget.27303](https://doi.org/10.18632/oncotarget.27303)
- [17] Zhang R, Zhu H, Yuan Y, et al. SPAG6 promotes cell proliferation and inhibits apoptosis through the PTEN/PI3K/AKT pathway in Burkitt lymphoma. *Oncol Rep.* 2020;44(5):2021–2030. doi: [10.3892/or.2020.7776](https://doi.org/10.3892/or.2020.7776)
- [18] Carnero A, Blanco-Aparicio C, Renner O, et al. The PTEN/PI3K/AKT signalling pathway in cancer, therapeutic implications. *Curr Cancer Drug Targets.* 2008;8(3):187–198. doi: [10.2174/156800908784293659](https://doi.org/10.2174/156800908784293659)
- [19] Chen H, Zhou L, Wu X, et al. The PI3K/AKT pathway in the pathogenesis of prostate cancer. *Front Biosci (Landmark Ed).* 2016;21(5):1084–1091. doi: [10.2741/4443](https://doi.org/10.2741/4443)
- [20] Lonergan KM, Chari R, Deleeuw RJ, et al. Identification of novel lung genes in bronchial epithelium by serial analysis of gene expression. *Am J Respir*



- Cell Mol Biol. 2006;35(6):651–661. doi: [10.1165/rcmb.2006-0056OC](https://doi.org/10.1165/rcmb.2006-0056OC)
- [21] Chen J, Wu Y, Luo X, et al. Circular RNA circRHOBTB3 represses metastasis by regulating the HuR-mediated mRNA stability of PTBP1 in colorectal cancer. *Theranostics*. 2021;11(15):7507–7526. doi: [10.7150/thno.59546](https://doi.org/10.7150/thno.59546)
- [22] Bray F, Ferlay J, Soerjomataram I, et al. Global cancer statistics 2018: GLOBOCAN estimates of incidence and mortality worldwide for 36 cancers in 185 countries. *CA A Cancer J Clin*. 2018;68(6):394–424. doi: [10.3322/caac.21492](https://doi.org/10.3322/caac.21492)
- [23] Miller KD, Nogueira L, Mariotto AB, et al. Cancer treatment and survivorship statistics, 2019. *CA Cancer J Clin*. 2019;69(5):363–385. doi: [10.3322/caac.21565](https://doi.org/10.3322/caac.21565)
- [24] Rubens RD. Metastatic breast cancer. *Curr Opin Oncol*. 1993;5(6):991–995. doi: [10.1097/00001622-199311000-00007](https://doi.org/10.1097/00001622-199311000-00007)
- [25] Solé C, Lawrie CH. Circular RNAs and cancer: opportunities and challenges. *Adv Clin Chem*. 2020;99:87–146.
- [26] Xia J, Wu C, Tang Y, et al. CircMYH9 increases KPNA2 mRNA stability to promote hepatocellular carcinoma progression in an EIF4A3-dependent manner. *Am J Cancer Res*. 2022;12(9):4361–4372.
- [27] Zheng X, Huang M, Xing L, et al. The circRNA circSEPT9 mediated by E2F1 and EIF4A3 facilitates the carcinogenesis and development of triple-negative breast cancer. *Mol Cancer*. 2020;19(1):73. doi: [10.1186/s12943-020-01183-9](https://doi.org/10.1186/s12943-020-01183-9)
- [28] Chan CC, Dostie J, Diem MD, et al. eIF4A3 is a novel component of the exon junction complex. *RNA (New York, NY)*. 2004;10(2):200–209. doi: [10.1261/rna.5230104](https://doi.org/10.1261/rna.5230104)
- [29] Zhang Z, Jones BH, Tang W, et al. Dissecting the axoneme interactome: the mammalian orthologue of Chlamydomonas PF6 interacts with sperm-associated antigen 6, the mammalian orthologue of Chlamydomonas PF16. *Mol & Cell Proteomics: MCP*. 2005;4(7):914–923. doi: [10.1074/mcp.M400177-MCP200](https://doi.org/10.1074/mcp.M400177-MCP200)
- [30] Altenberger C, Heller G, Ziegler B, et al. SPAG6 and L1TD1 are transcriptionally regulated by DNA methylation in non-small cell lung cancers. *Mol Cancer*. 2017;16(1):1. doi: [10.1186/s12943-016-0568-5](https://doi.org/10.1186/s12943-016-0568-5)
- [31] Ji Y, Jiang J, Huang L, et al. Sperm-associated antigen 4 (SPAG4) as a new cancer marker interacts with Nesprin3 to regulate cell migration in lung carcinoma. *Oncol Rep*. 2018;40(2):783–792. doi: [10.3892/or.2018.6473](https://doi.org/10.3892/or.2018.6473)
- [32] Zeng X, Xu W, Tong J, et al. SPAG5 as a novel biomarker and potential therapeutic target via regulating AKT pathway in multiple myeloma. *Leukemia & Lymphoma*. 2022;63(11):2565–2572. doi: [10.1080/10428194.2022.2086247](https://doi.org/10.1080/10428194.2022.2086247)
- [33] Xiao G, Xu X, Chen Z, et al. SPAG5 expression predicts poor prognosis and is associated with adverse immune infiltration in lung adenocarcinomas. *Clin Med Insights Oncol*. 2023;17:11795549231199915. doi: [10.1177/11795549231199915](https://doi.org/10.1177/11795549231199915)
- [34] Gao X, Bu H, Gao X, et al. Pan-cancer analysis: SPAG5 is an immunological and prognostic biomarker for multiple cancers. *Faseb J*. 2023;37(10):e23159. doi: [10.1096/fj.202300626R](https://doi.org/10.1096/fj.202300626R)
- [35] Zhu C, Menyhart O, Györfy B, et al. The prognostic association of SPAG5 gene expression in breast cancer patients with systematic therapy. *BMC Cancer*. 2019;19(1):1046. doi: [10.1186/s12885-019-6260-6](https://doi.org/10.1186/s12885-019-6260-6)
- [36] Xiao C, Li M, Huang Q, et al. SPAG9 promotes prostate cancer proliferation and metastasis via MAPK signaling pathway. *Am J Transl Res*. 2019;11(8):5249–5260.
- [37] Luo S, Ren B, Zou G, et al. SPAG9/MKK3/p38 axis is a novel therapeutic target for liver cancer. *Oncol Rep*. 2019;41(4):2329–2336. doi: [10.3892/or.2019.6987](https://doi.org/10.3892/or.2019.6987)
- [38] Zhu Q, Zhang X, Zai HY, et al. Hu Y: circSLC8A1 sponges miR-671 to regulate breast cancer tumorigenesis via PTEN/PI3k/Akt pathway. *Genomics*. 2021;113(1):398–410. doi: [10.1016/j.ygeno.2020.12.006](https://doi.org/10.1016/j.ygeno.2020.12.006)
- [39] Zhan CH, Ding DS, Zhang W, et al. The cancer-testis antigen a-kinase anchor protein 3 facilitates breast cancer progression via activation of the PTEN/PI3K/AKT/mTOR signaling. *Bioengineered*. 2022;13(4):8478–8489. doi: [10.1080/21655979.2022.2051687](https://doi.org/10.1080/21655979.2022.2051687)
- [40] Yin J, Li X, Zhang Z, et al. SPAG6 silencing induces apoptosis in the myelodysplastic syndrome cell line SKM-1 via the PTEN/PI3K/AKT signaling pathway in vitro and in vivo. *Int J Oncol*. 2018;53(1):297–306. doi: [10.3892/ijo.2018.4390](https://doi.org/10.3892/ijo.2018.4390)